PERFORMANCE OF AIRBUS ROBOTIC TELESCOPE AND THE SST DATA PROCESSING FRAMEWORK SPOOK

Giovanni Cirillo[(1)], Maria G.V. Dimitrova[(1)], Jens Utzmann[(1)], Yannick Heinz[(1)], Guido Pedone[(1)], David Vallverdu Cabrera[(1)]

[(1)]Airbus Defence and Space GmbH, Claude-Dornier Straße 88090 Immenstaad Germany,
email: {giovanni.cirillo,jens.utzmann}@airbus.com

ABSTRACT

The Special Perturbations Orbit determination and Orbit analysis toolKit (SPOOK) is a versatile software framework developed at Airbus Defence and Space, with the aim to support Space Surveillance and Tracking (SST) activities. The core characteristics of SPOOK were introduced in 2018 [10]. This paper will present the improvements and new features that have been integrated into SPOOK since then, and will give an updated high-level breakdown of its functionalities. Many of these new functionalities have been tested also with real data, mainly from Airbus Robotic Telescope (ART), a 40 cm aperture optical telescope located in Extremadura, Spain. This paper will present the level of accuracy that can be obtained with SPOOK as well as a summary of the observations performed so far, including statistics per orbital region.

1 GENERAL INTRODUCTION

The space debris population around the near-Earth space environment is continuously increasing, and is expected to grow further unless strong mitigation is implemented in the near future [3, 18]. To enable such mitigation strategies so that hazards derived from space debris overpopulation may be prevented, it is necessary to understand the characteristics of the space debris population itself. Thus, Space Surveillance and Tracking (SST) capabilities are the key to guarantee sustainable future for the space sector.

The Security in Space team of Airbus Defence and Space develops its own SST software framework called the Special Perturbations Orbit determination and Orbit analysis toolKit (SPOOK), already introduced in [9, 11], which focuses on space object catalogue generation and maintenance. Furthermore, Airbus Defence and Space owns and operates the Airbus Robotic Telescope (ART), a 40 cm aperture optical telescope. With the introduction of ART, it was possible to thoroughly test and validate SPOOK's capabilities with real-world data. SPOOK and ART together form the core of the SST pipeline, and they are used in conjunction on a daily basis to produce and process SST observations, as well as to enable other SST-related activities. This paper describes the incremental upgrades that have been added into SPOOK and ART since 2018. Section 2 opens with an overview of the background of SPOOK previous to this paper. It is followed by an overview of ART in section 3. Then, section 4 summarizes all the features that SPOOK has received since 2018, from the point of view of the maintenance of a space catalogue. The paper finishes with section 5, where it presents the performance statistics of these new upgrades, together with the statistics of the data generated using SPOOK and ART during the past two years.

2 BACKGROUND OF SPOOK

This section is a summary of the status of SPOOK previous to the work presented in this paper. The previous capabilities of SPOOK included [10]:

- A simulation layer that can simulate optical and radar astrometric measurements, based on object ephemeris propagation plus simulation of sensor characteristics.
- An analysis layer which includes orbit determination, initial orbit determination and uncertainty propagation, together with statistical measurement analysis w.r.t. observability criteria.
- An interface layer that can read and write input and output in several standard and proprietary formats.

These capabilities had been validated mainly with simulated data.

3 AIRBUS ROBOTIC TELESCOPE OVERVIEW

ART is a 40cm aperture telescope deployed in June 2018 in Extremadura (Spain) by Airbus Defence and Space for SST [16]. It is equipped with a CCD detector and, since 2020, with an Ultraviolet Blue Visible Red Infra-red (UBVRI) filter wheel.

ART is capable of performing automated optical observations of space objects from Low Earth Orbits (LEO) to Geostationary Earth Orbits (GEO). Furthermore, with its wide Field of View (FOV), ART can perform surveillance observations in order to discover new objects. Different surveys strategies have

Proc. 8th European Conference on Space Debris (virtual), Darmstadt, Germany, 20–23 April 2021, published by the ESA Space Debris Office
Ed. T. Flohrer, S. Lemmens & F. Schmitz, (http://conference.sdo.esoc.esa.int, May 2021)

already been implemented and tested.

The telescope can also be used to observe tumbling objects to study their light curves, as successfully demonstrated in the ESA SST Sensor Data Acquisition study [16].

Furthermore, thanks to its astronomical observations of celestial bodies such as the interstellar comet *C2019Q4 Borisov* (with an apparent magnitude around 17) in December 2019, ART has been added into the list of observatories of the Minor Planet Center (MPC) of the International Astronomical Union (IAU) [7].

Since its deployment, the Airbus sensor has been used for internal Research and Development and for international SST projects and studies.

The integration of ART into the SST software framework SPOOK [10] has enabled the development and validation of an end-to-end processing pipeline. The system is a fundamental ground-based test-bed for future development of space-based systems and it has a proven central role in fostering cooperation within the SSA community [16], thanks to its participation in international and national studies such as the NATO “Collaborative Space Domain Awareness Data Collection and Fusion Experiment”.

Figure 1. Airbus Robotic Telescope

4 NEW INTEGRATIONS INTO SPOOK

4.1 Preparation of the observations

The first necessary step for an SST system is to collect measurements of Resident Space Objects (RSO). These measurements can be obtained through observations of RSOs made by various sensors or sensor networks. The observation methodologies can be various depending on both the characteristics of the observer (e.g. type, location, physical properties, etc.) and RSO to be observed.

Generally speaking, it is the aim of SST to create and maintain a catalogue of RSOs; therefore the observation strategies are generated so as to follow exactly these two aspects: catalogue generation and catalogue maintenance.

This section will present the upgrades made on the observation planning capability in SPOOK since the last presentations in [10, 16], focusing on the two main aforementioned planning methodologies.

Catalogue Generation

Survey observation plans are generated without knowing the positions of RSO beforehand. To accomplish this task, for the GEO satellites, SPOOK has integrated the so called “GEO fence scenario”.

Fig. 2 shows in blue the orbit of a sample GEO catalogue retrieved from Space-track [15] and propagated for 1 day. The red line indicates the fitting line of this RSO distribution. The black circle is the position of the Earth shadow as of 17th March 2021 at 20:17.

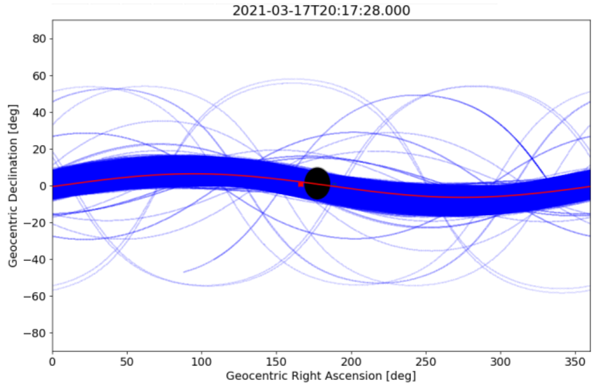

Figure 2. Geosynchronous belt example

An initial design for a fence strategy was presented in [10], and the GEO fence scenario integrated in SPOOK was described in [9].

Following the description in [9], the GEO fence scenario allows the user to distribute a series of survey fences along the right ascension coordinate. Each fence can be spread in the declination coordinate by a desired number of fields. An example of this plan is presented in Fig. 3. In this particular survey plan a strategy with 4 fences and 4 fields (green blocks) has been adopted. The fences are placed close and symmetrically to the Earth shadow (black circle) to allow better illuminance conditions of the objects, and centred at constant declination or adapted to increase the probability of detecting an inclined object.

This scenario allows, eventually, the revisit of RSOs during their orbital motion from one fence to another. The number of fields defines the coverage of the RSOs at different declinations and thus different inclinations of the orbits. The plan can be generated to be leak proof. Depending on the dynamical model of the sensor, in fact, a leak proof plan is a plan where the observer performs a survey of all the fences (and fields) in less time than an object takes to cross one fence.

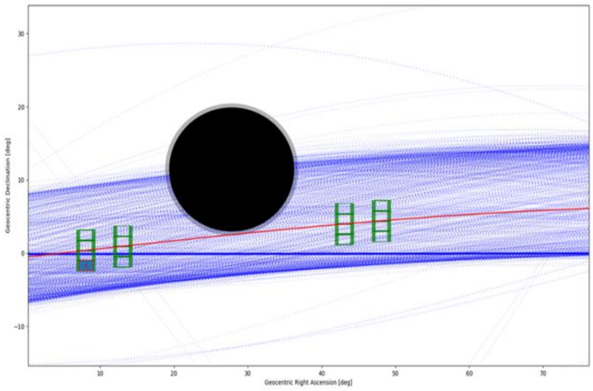

Figure 3. Caption from the variable GEO fence scenario visualization tool

Catalogue Maintenance

The maintenance of a catalogue corresponds to the tracking requests that can be sent to a sensor or network of sensors. When the orbit of the object is known, the catalogue maintenance sensor tasking is taking care of maintaining the information of such objects within a certain level of uncertainty envelope. The optimization strategies necessary to maximize certain objectives like coverage, follow-up, information gain, etc. fall into this framework.

Within SPOOK, three are the main observation strategies for catalogue maintenance. The design of an observation strategy, in this sense, starts with the definition of a certain objective function, and then with the formulation of a proper optimization method to maximize it.

The three methods can be described in this way:

1. Greedy-method: the objective function is the benefit directly related with a certain observation request and can be tuned accordingly to special interest in observing that specific satellite, maximum coverage (tracking a different object every time), slewing time or angular distance from the previous task. The optimization method involves a dynamic programming strategy as in [5, chapter 12].
2. Heuristic methods (like the genetic algorithm): they can be used to maximize a covariance-based objective function. In this case the objective function takes into account the information gain obtained after a certain observation task and a genetic algorithm method tries to optimize it for the whole observation night.
3. Automatic scheduler: a baseline implementation for a real-time tracking strategy has been recently integrated into SPOOK. The presentation of this strategy is given in [8]. In this case, the sensor tasking optimization is performed step-by-step and not offline as the previous two methods. At every observation step the scheduler selects the observation request with the highest reward function that expresses the information gain between the predicted multi-object posterior density and the future updated posterior density.

Additionally to the generation of a maintenance tracking-plan for a given catalogue of objects, those scheduling strategies can cope, also, with different SST scenarios:

- Calibration scenario: for each observation night a sensor should produce a calibration tracking plan to assess the fidelity of the data of the whole observation. SPOOK offers the possibility to create at determined time slots (usually at the beginning and at the end of the night) a calibration plan. This plan is done with objects that have a well-known ground truth or photometric properties as navigation satellites like GPS, Galileo constellation, ILRS (International Laser Ranging Station) targets or even specific stars. This scenario is performed with a simply greedy method that maximizes the number of observed objects.
- Light curves tracking: for object characterization purposes, there could be the necessity to observe for long period for reasons other than Orbit Determination (OD). Similarly to before, a greedy method schedules observations for these particular targets for an observation night.

4.2 Pre-Processing and Image Processing

The raw images collected during ART observation campaigns are reduced with the use of the external image processing software Astrometry24.NET (A24N) developed by Sybilla Technologies [14]. Before the image processing step, the images are pre-processed to verify that they are suitable for the following stages.

Additionally an optional filtering of the images can be done based on a preliminary estimation of the SNR or based on the Analogue to Digital Unit values of the images. This is useful before the photometric calibration step for several reasons, for instance the detection of images with saturated pixels.

4.3 Post-Processing

Tracklet Linking

Tracklet linking is the step when the measurements obtained in the image processing are linked to each other if they belong to the same object. Tracklet linking performance is highly affected by the number of false positives per image, but it is possible to filter most of them using their photometric properties (e.g. too low SNR). After this step, several possible tracklet candidates are generated based mainly on geometrical constraints (a crossing of an object is usually short compared to the orbital period, so the arc can be easily approximated as a straight line, as the blue line in Fig. 4). A challenging case occurs when LEO objects are observed, because their relative velocity could be very high with respect to a ground observer. As it appears clear in the red line in Fig. 5, the linear approximation in this case is not applicable anymore and a higher degree approximation of the tracklet shape plus a proper rotation of the reference frame is used.

In both Fig. 4 and Fig. 5 the grey dots are the false positives that are removed in the pre-filter step or during the generation of the possible candidates.

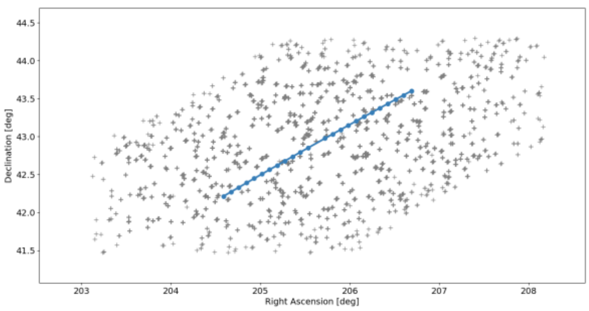

Figure 4. Tracklet linking of a GPS satellite

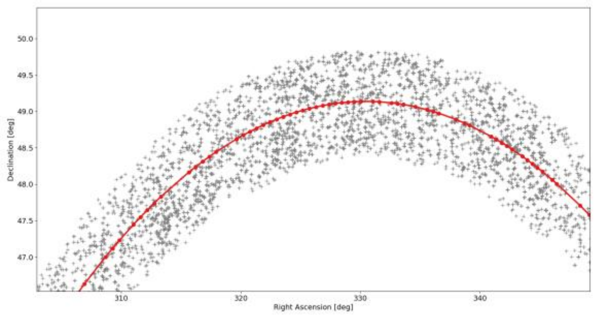

Figure 5. Tracklet linking of a LEO satellite

Among all the generated candidates, only the ones with at least 4 measurements are considered reliable, the others are considered fake tracklets and discarded.

Currently SPOOK is able to perform tracklet linking not only for optical sensors (like ART) but also for other common types of SST sensor, like Radar, Doppler-Radar or Laser-Ranging.

Correlation

In the data association framework, Tracklet-to-Object Correlation is the ability to associate each tracklet to an object inside a pre-existent catalogue. When this association is not successful and the tracklet alone is not sufficiently representative of an orbit to trigger correctly an Initial Orbit Determination (IOD) estimator, the Tracklet-to-Tracklet Correlation tries to correlate it with other tracklets generated by the same objects. A description of the Tracklet-to-Object Correlation method and its integration inside SPOOK are given in [11]. Both Tracklet-to-Object Correlation and Tracklet-to-Tracklet Correlation start with the definition of an attributable-vector from observations. The total number of possible orbital candidates is then pre-filtered accordingly to certain physical and orbital constraints (e.g. negative total energy, constrained eccentricity or semi-major axis, etc.), with the definition of a Constrained Admissible Region (CAR), with a process similar to the one described in [2]. Finally for Tracklet-to-Object Correlation a highest likelihood association is used to associate the tracklet to an object of which robust a priori information was available. Tracklet-to-Tracklet Correlation instead compares the CAR of the first attributable-vector with the CAR generated by a second tracklet. However, the literature [4] suggests waiting for a third tracklet association to confirm the correlation and avoid false associations.

Astrometric Calibration

Astrometric calibration is the step when the accuracy of a sensor can be estimated. A comparison between the obtained measurements and a reliable ephemerides source is performed. For only few objects a reliable source is available. The main sources are the NASA SP3-c (Standard Product 3) files where position state vectors and covariances are provided with a 15-minutes time gap, available only for the GPS satellites. Other important sources are the satellites tracked by ILRS, for which CPF (Consolidated Prediction Format) files are provided. This list of satellites includes the Galileo and the GLONASS constellations, plus 30-40 objects distributed in all the orbital regions from LEO to GEO. This list is continuously updated because some new satellites trackable by ILRS are launched and some others are dismissed.

The distribution of the residuals as a function of time, number of matched stars in the image, SNR or aspect ratio (which represent the oblateness of the object in the image) could give an indication of the impact of these quantities on the residual values. Normally the number of matched stars and the SNR are the parameters that affect the residuals the most – the former because it alters the astrometric reduction, the latter because it affects the accuracy of the object centroid.

As example, in Fig. 6 the residual values in right ascension and declination from several GPS satellites observed by ART during the night between 13th and 14th March 2021 are shown as a function of the number of matched stars. It is clear that images with less than 50 matched stars give residuals that are even 1 order of magnitude higher than with more stars. The measurements taken from these images can be therefore removed from the pipeline after the images processing.

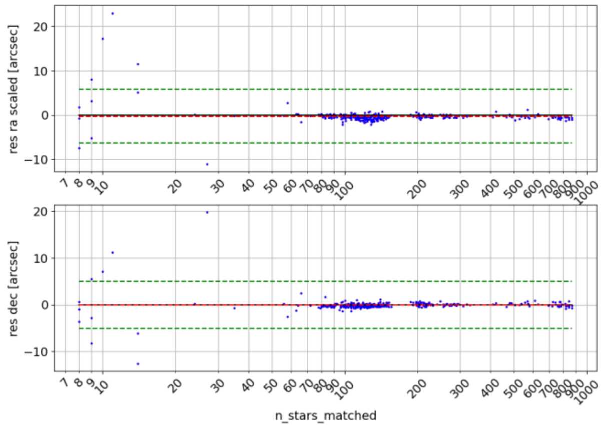

Figure 6. Residuals vs number of matched stars

Orbit Determination

Orbit Determination (OD) improves the estimation of an object whenever new measurements of that object are available. Several methods are currently implemented in SPOOK and tested with simulated measurements:

- Sequential methods: Extended Kalman Filter (EKF), Unscented Kalman Filter (UKF), Unscented-Schmidt Kalman Filter (USKF).
- Batch methods: Weighted Least Squares (WLS), Sequential-Batch WLS (or SBWLS).
- Advanced methods, based on the sequential ones: Gaussian Mixtures EKF (GMEKF), Gaussian Mixtures UKF (GMUKF) with constant number of kernels, and their adaptive version starting with 1 kernel and change the number of kernels on the fly, whenever a split or merge seems appropriate.

Initial Orbit Determination

When the measurements are enough to support orbit estimation, Initial Orbit Determination (IOD) is performed within SPOOK. The measurements can come from a long tracking campaign of an object or several tracklets that have been correlated each other.

The general approach for IOD is divided into two steps: a first orbital estimation and a WLS reduction (or refinement) of the orbit. The orbital estimators are wide in the literature; SPOOK in particular makes use of two classical methods: a circular orbit estimator as proposed in [1], and the general Gauss method.

4.4 Services

Photometric Analysis

SPOOK has recently incorporated object characterization capabilities by exploiting the photometric data extracted from optical measurements – i.e. light curves.

On the one hand, SPOOK has a new module which implements common signal processing techniques, such as Fourier analysis (including the Lomb-Scargle periodogram) signal autocorrelation. This new set of capabilities allows analysing the periodic behaviour of light curves, which leads to the implementation of the epoch method, used to estimate the sidereal axis and period of an object rotating around a principal axis in steady state. E.g., Fig. 7 shows the phase plot of a light curve of the ISO satellite measured on the morning of 2019-10-06 by ART (blue triangles), which fits a Fourier series with four harmonics (black line) whose fundamental period is $1/33.51$ s [17].

On the other hand, SPOOK has been upgraded with tools to represent object shapes and their reflectance surface properties as arbitrary polyhedrons in 3D space, which has enabled to:

1. simulate light curves, as an extension to the classical sensor simulation layer of SPOOK;
2. implement convex shape estimation from light curves, when attitude is known, via the Extended Gaussian Image representation of a convex polytope [9].

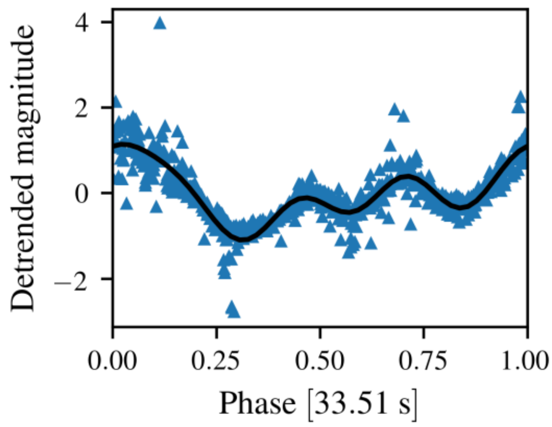

Figure 7. Phase plot of the ISO satellite

Image Visualization

SPOOK allows the fast visualization of FITS[1] images obtained after an observation campaign. The image visualization tool allows the user to apply some of the cataloguing refinements directly to raw images (and measurements) in order to visualize directly some of the

[1] Flexible Image Transport System (FITS) is a standard digital format mainly used by astronomers for data interchange and archiving format.

features of interest. Examples are given in Fig. 8 and Fig. 9, for a tracking and survey campaign respectively. In Fig. 8 in the centre the Tracklet-to-Object correlated GPS satellite is highlighted in red; in yellow are visible, eventually, false measurements that did not succeeded the tracklet linking association. In Fig. 9 more objects have been associated to tracklets using tracklet linking and then correlated with the catalogue.

Figure 8. Caption from the output of the visualization tool of a tracking campaign done by ART.

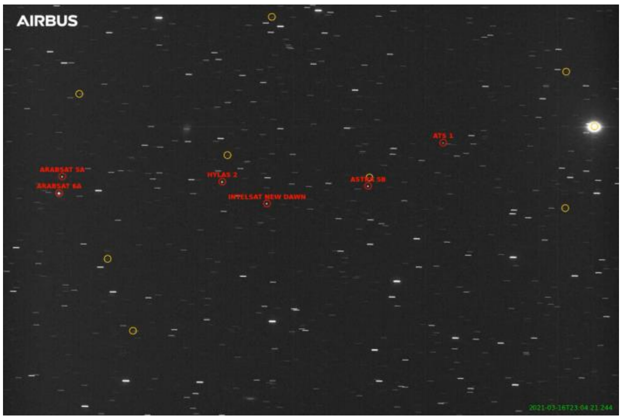

Figure 9. Caption from the output of the visualization tool of a variable GEO fence campaign done by ART.

Database and Cataloguer

SPOOK's cataloguing system is able to handle information from various sources like: internal or external measurements and internal or external catalogues of objects. In particular, it makes use of automatic services to daily:

- fetch object data from external catalogues, like the space-track TLE and Special Perturbation (SP) vectors;
- produce an observation plan for the sensors present inside the observer table in the database;
- execute the cataloguing pipeline routines (from tracklet linking to orbit determination).

Manoeuvre Simulation and Estimation

To further account for realistic SSA scenarios within SPOOK, its orbit propagation and sensor simulator capabilities have been extended to account for arbitrary manoeuvres. SPOOK can be configured with arbitrary 3D acceleration vs. time profiles, which allows representing any kind of manoeuvre, from impulsive burns to low electrical thrust transfers.

Furthermore, SPOOK incorporates the capability to estimate the characteristics of a manoeuvre between two separate orbital states, which shall be used as an eventual metric to determine whether separate measurements and/or catalogue objects actually belong to the same space object that has undergone a manoeuvre or not.

Fig. 10 shows the conceptual representation of the trajectory optimization of SPOOK, where the satellite on the left represents the initial state, whereas the yellow satellite on the right represents the final state. The algorithm optimizes the acceleration profile for minimal fuel consumption, with the boundary condition that the final state of the calculated trajectory (blue satellite on the right) equals the actual final state. The sensor is represented by ART in the middle.

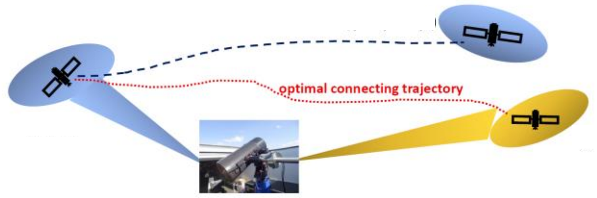

Figure 10. Conceptual representation of the manoeuvre trajectory optimization adapted from [6].

Conjunction Assessment

A recent integration inside Airbus' software tool is the conjunction assessment. It has been presented in [9] and described in details in [12, 13]. The conjunction analysis is a tool that makes use of the SPOOK analysis and propagation routines to perform a conjunction assessment between two lists of satellites. The first can be understood as a list of operative assets of a space operator, while the second can be the complete catalogue of space objects.

5 PERFORMANCE RESULTS

5.1 Data Acquisition Campaigns

As SST sensor, ART has participated in several European, national and international observation campaigns. Between 2019 and 2020, the majority of the observation time has been dedicated to the ESA SST Sensor Data Acquisition activity.

During the project, ART has conducted tracking in LEO, MEO (Medium Earth Orbit), GEO and HEO (Highly Elliptical Orbit), multiple surveillance strategies (GEO fence and GEO belt survey scanning) and tumbling object observations.

In total the campaign saw 118 nights of observations being performed. The tracking campaign led to the collection of more than 2700 correlated TDMs for 662 different targets in all orbital regions. The breakdown in orbital regions of the tracking targets observed is shown in Tab. 1.

Table 1. Summary of targets observed during ESA SST Sensor Data Acquisition tracking campaign

Sensor	Regimen	N. of targets	N. of observation nights
ART	LEO	160	65
	MEO	263	118
	GEO	239	58

On the other hand, the survey campaign has proven more prolific. It has run over a total of 40 nights and has been divided in 7 stages. After a first test phase several survey strategies were explored and implemented, this allowed planning the following 4 stages of GEO fence surveillance scenarios so to achieve optimized revisit rates of the targets while maximizing the number of objects observed. The campaign ended with a GEO belt survey scan pattern, hence observing repeatedly the belt over the nigh starting from the lowest right ascension reachable by the telescope and proceeding to the maximum reachable.

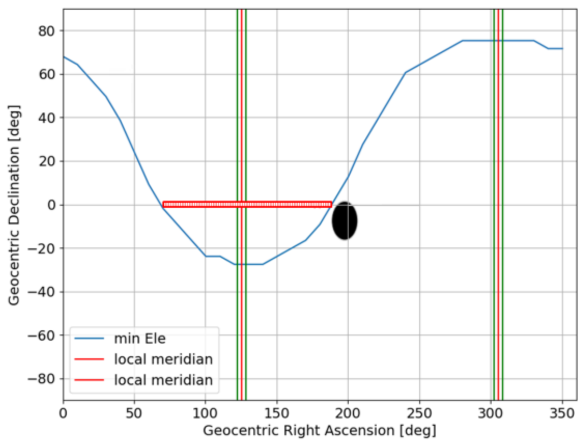

Figure 11. Depiction of the GEO belt scan survey strategy

In total 8184 TDMs have been delivered of which 6209 were successfully correlated to GEO objects from the Space-Track catalogue (see Tab. 2).

Table 2. Summary of the data collected for ESA SST Sensor Data Acquisition study during the survey campaign

Observation Stategy	N. Days	N. TDM linked	N. TDM correlated
Survey Test phase	8	431	321
2 fences 1 field	5	1413	971
2 fences 1 field GEO belt adaptation	7	1819	1212
4 fences 1 field	8	1974	1672
4 fences 1 field GEO belt adaptation	4	134	72
GEO belt scan	8	2413	1961

A similar success was reached with the observation of LEO targets for photometric studies (see Tab. 3). Several targets were selected chosen for their known tumbling motion. LEO observations are usually challenging due to the low altitude and high angular rates that the telescope has to match to track them on their orbit.

Table 3. Targets observed for light curve analysis within the ESA SST Sensor Data Acquisition study

Target	Date	N of images
VESPA 2013-021D	20/03/2019	110
ISO 1995-062A	06/10/2019	930
ISO 1995-062A	06/12/2019	330
ERS 1 1991-050A	05/07/2019	644
ERS 1 1991-050A	29/06/2019	500
ERS 1 1991-050A	15/07/2019	200
ERS 1 1991-050A	16/07/2019	160

Overall, since the new integrations in SPOOK have been added to the pipeline, ART has collected more than 268k images in tracking mode (see Tab. 4). This includes also the tumbling objects used for light curves estimation and low LEO satellites, both active ones such as the Starlink constellation and debris.

Table 4. Overview of the images collected by ART since 2019 divided per orbital region

Observation mode	N. images
LEO TRK	41399
MEO TRK	68721
GEO TRK	36371
GEO SRV	82116

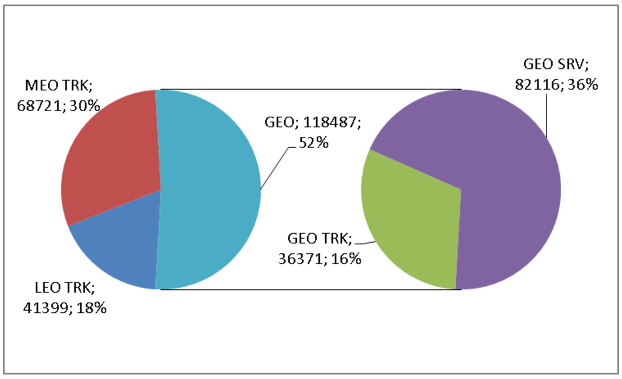

Figure 12. Graphical representation of Tab. 4

Additional 131k images have been collected with various survey strategies, including conjunctions, GEO fence and survey scan mode.

These images include various observation campaigns, as well as for internal development and for the population of an internal catalogue.

5.2 Astrometric Calibration

In terms of calibration, complete results for the three years of operation of ART are shown in Tab. 5.

The results are consistent over the time span and show the high accuracy of the sensor and its suitability for SSA observation campaigns. The results for 2021 show a little improvement as a result of the upgrade of the processing pipeline and in particular of the image processing software.

Table 5. Calibration results for ART since 2019

Year	N meas.	RA mean (arcsec)	DEC mean (arcsec)	RA sigma (arcsec)	DEC sigma (arcsec)
2019	3376	-0.065	-0.053	0.487	0.465
2020	23352	-0.056	-0.054	0.490	0.505
2021	4610	-0.089	-0.062	0.372	0.392

For example, Fig. 13 shows the residuals in right ascension and declination for 347 measurements of 5 different GPS satellites observed by ART during the night between 13th and 14th March 2021, compared to the sp3 "ground truth". To take into account the distortion due to the spherical coordinates, the residuals in right ascension are scaled by the cosine of the declination [19]. The dashed red line represents the mean of all the residuals, whereas the green dashed lines represent the 3-standard deviation envelope. Only five outliers are identified, whose value is anyway in the range ±2 arcsec. The sensor accuracy (defined as 1-sigma standard deviation) for this set of measurements is below 0.4 arcsec (so in the sub-pixel region), in line with the overall statistics for 2021.

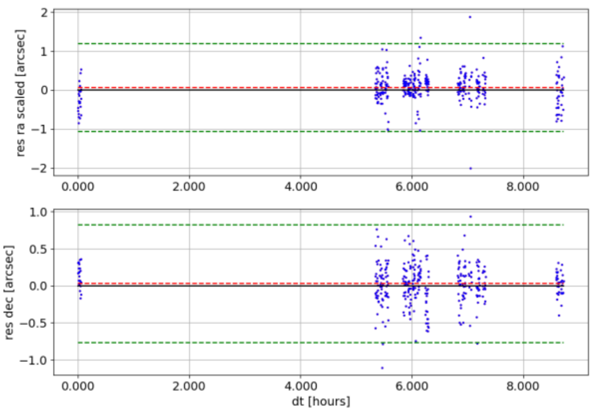

Figure 13. Example of residual plot for GPS satellites observed by ART

A quantile plot (Q-Q plot, Fig. 14) is used to visually show the normality of the residuals by comparing the sample quantiles (real residuals) with the theoretical quantiles (Gaussian distribution with same mean and standard deviation of the residuals). If the points in the Q-Q plot lay close to the 45 degrees line (red line) it means that the residuals follow a normal distribution (the outliers are the points that largely deviate from the red line). An alternative plot that can be used for this purpose is the P-P plot (Fig. 15) where the quantiles are substituted by the cumulative distribution functions. The disadvantage of the latter plot is that the outliers are not clearly identifiable.

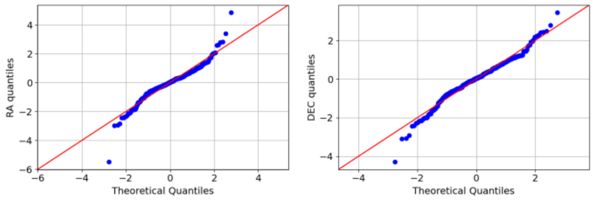

Figure 14. Example of Q-Q plot residuals for GPS satellites observed by ART

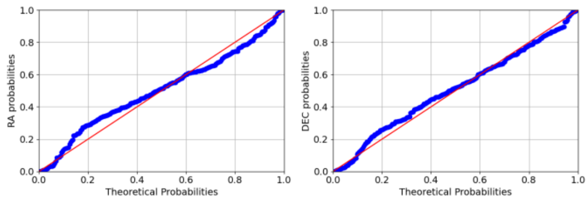

Figure 15. Example of P-P plot residuals for GPS satellites observed by ART

5.3 Orbit Determination

To show the performance of the OD tool, an exemplary case of a GPS satellite is shown.

Fig. 16 and Fig. 17 show the OD results of a GPS satellite observed the 9th, 13th and 14th March 2021 using Extended Kalman Filter and Weighted Least Squares. The red line in the plots shows the 3-standard deviation, whereas the blue line shows the “true” error using the sp3 files as reference. The vertical lines are placed where new measurements are available. The plots show only the tangential component of the position (the component of the state vector that usually gives the highest error since it is in the direction of the velocity vector). For EKF the initial covariance is chosen arbitrarily high (it drops immediately after the first measurements) and process noise is added and tuned to take into account unmodelled perturbations. For WLS no prior information about the covariance is required, but in typical cases the covariance is underestimated because no process noise can be added using this method (however in this exemplary case the covariance fits the error well). The 3-standard deviation at the time of the last measurement is under 30 metres for EKF and under 40 metres for WLS (in the other directions is even lower). The true error tends to follow the same pattern as the 3-standard deviation, but with a smaller scale: for EKF it grows during the propagation and drops whenever new measurements are available; for WLS it has a periodic behaviour with similar phase. The addition of the process noise in the EKF guarantees that the filter does not saturate and that the solution converges to the real one.

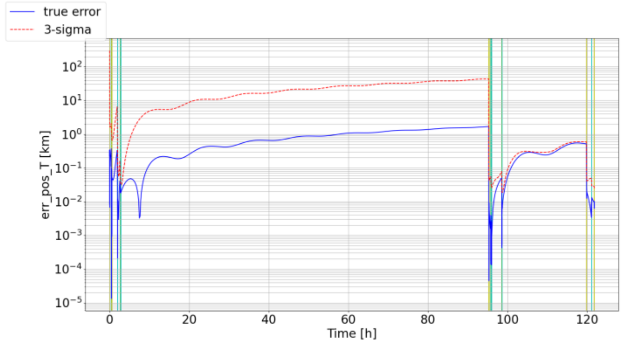

Figure 16. EKF OD plot for a GPS satellite observed by ART

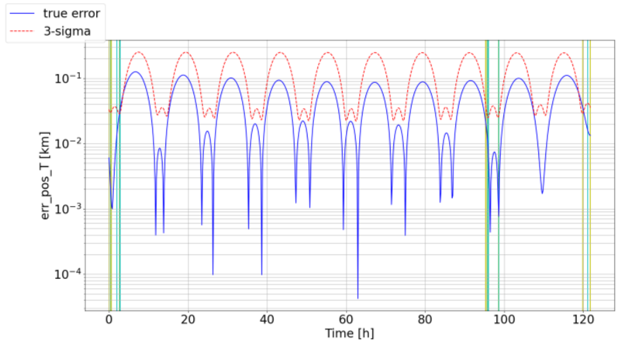

Figure 17. WLS OD plot for a GPS satellite observed by ART

6 CONCLUSIONS

ART and SPOOK represent Airbus’ end-to-end SST observation and processing capability. Together they have been validated through numerous campaigns and proven their relevance for SSA studies. ART allows observations in every orbital region alongside astronomical observations. SPOOK is a processing tool that can be used for different types of SST sensors and whose functionalities have been validated and improved through ART operation.

This paper has shown the new tools and services developed within SPOOK and it has demonstrated their extent and capabilities. The software is continuously developed to add new features and improve the current ones.

7 REFERENCES

1. Beutler, G. (2010). Methods of Celestial Mechanics I: Physical, Mathematical and Numerical Principles, 2. In *Methods of Celestial Mechanics I: Physical, Mathematical and Numerical Principles, 2* (p. 369).

2. DeMars, K. J., & Jah, M. K. (2013). Probabilistic initial orbit determination using Gaussian mixture models. *Journal of Guidance, Control, and Dynamics*, *36*(5), 1324--1335.

3. (2020). *ESA's Annual Space Environmental Report.* ESA Space Debris Office.

4. Farnocchia, D., Tommei, G., Milani, A., & Rossi, A. (2010). Innovative methods of correlation and orbit determination for space debris. *Celestial Mechanics and Dynamical Astronomy, 107*(1), 169--185.

5. Goodrich, M. T., & Tamassia, R. (2015). *Algorithm Design and Applications.*

6. Jaunzemis, A. D., Mathew, M. V., & Holzinger M. J. (2015). Metric Maneuver Detection with Gaussian Mixtures and Real Data.

7. *List Of Observatory Codes*. (n.d.). (The International Astronomical Union, Minor Planet Center) Retrieved 04 07, 2021, from https://www.minorplanetcenter.net/iau/lists/ObsCodesF.html

8. Pedone, G., Utzmann, J., & Förtstner, R. (2021). Baseline Algorithm Definition for a Future Real-Time Autonomous Sensor Scheduling Strategy for SST. *8th European Conference on Space Debris 2021.* ESA/ESOC, Darmstadt, Germany.

9. Pedone, G., Vallverdu Cabrera, D., Dimitrova Vesselinova, M. G., Cirillo, G., Heinz, Y., Schiemenz, F., & Utzmann, J.. (2021). SPOOK: a Tool for Space Objects Catalogue Creation and Maintenance Supporting Space Safety and Sustainability. *IAA/UT 7th STM Conference 2021.* Austin, TX, USA.

10. Rodriguez Fernandez, O., Utzmann, J., & Hugentobler, U. (2018). SPOOK – A comprehensive Space Surveillance and Tracking analysis tool. *Acta Astronautica 158*, 178-184.

11. Rodriguez Fernandez, O., Utzmann, J., & Hugentobler, U. (2019). Correlation of Optical Observations to Catalogued Objects using Multiple Hypothesis Filters. *1st NEO and Debris Detection Conference.*

12. Schiemenz, F. (2019). Survey of the operational state of the art in conjunction analysis. *CEAS Space Journal*.

13. Schiemenz, F. (2020). *PhD Dissertation: Covariance and Uncertainty Realism for Low Earth Orbiting Satellites via Quantification of Dominant Force Model Uncertainties.* University of Würzburg.

14. Sibilska, A., Kozlowski, S., Sybilski, P., et al. (January 2019). Astrometry24.NET - precise astrometry for SST and NEO. *ESA 1st NEO and Debris Detection Conference.* Darmstadt.

15. Squadron, S. C. (n.d.). *space-track*. (SAIC) Retrieved 03 17, 2021, from https://www.space-track.org/

16. Utzmann, J., Dimitrova Vesselinova, M. G., & Rodriguez Fernandez, O. (2019). Airbus Robotic Telescope. *1st NEO and Debris Detection Conference.* ESA Space Safety Programme Office.

17. Vallverdu Cabrera, D., Utzmann, J., & Förstner, R. (2021). Integration of Attitude Characterization in a Space Debris Catalogue using Light Curves. *8th European Conference on Space Debris 2021.* ESA/ESOC, Darmstadt, Germany.

18. Virgili, B. B. (2016). DELTA Debris Environment. *Proceedings of the 6th International.*

19. Ward, E., & Carbott, G. (2016). On Directional Measurement Representation in Orbit Determination. *AIAA/AAS Astrodynamics Specialist Conference.*